Power Converter for Use in Quasi-Wireless Capacitive Power Robotic Systems with Secondary Side Sensing and Switching

Carson Pope*†, Darren Boyd‡, Charles Van Neste*

*Electrical and Computer Engineering
†Center for Energy System's Research (CESR)
Tennessee Technological University
Cookeville, TN, United States
cdpope42@tntech.edu, cvanneste@tntech.edu
‡United States National Aeronautics and Space Administration (NASA)
Marshall Space Flight Center
Hunstville, AL, United States
darren.r.boyd@nasa.gov

***Abstract*—Presented is a novel approach to regulating voltage in a Quasi-Wireless Capacitive (QWiC) Power Transfer system for robotics. The method modifies traditional regulator topologies to isolate from the Quarter-Wave Resonator (QWR). Uniquely, this approach enables full secondary side sensing and regulation without needing feedback to the primary coil. A transistor-based circuit connects the smoothing capacitor to the input during charging and disconnects during discharging, ensuring output regulation. This design allows a micro-controller on the load side to control the transistor states. The use of a high value capacitance, typically in the range of a few farads allows the system to retain charge even during external loss of power much like a "battery-bank". Experimental results demonstrate stable voltage regulation with future work focusing on establishing design guidelines and optimizing control signal duty cycles for efficiency. Overall, this approach offers a promising solution for stable voltage regulation in QWiC-based robotic systems.**

I. Introduction

Wireless power transfer (WPT) finds diverse applications spanning transportation, biomedical, consumer electronics, and numerous other sectors [1]. Some forms are even being tested in challenging environments, such as autonomous underwater vehicles [2]. Among the various WPT forms, Quasi-Wireless Capacitive (QWiC) power transfer stands out, as it offers a way to transfer power over large conductive surfaces without a physical return wire. QWiC technology has demonstrated its use in personal mobility vehicle charging, robotics, and sensors [3]. In particular, QWiC's application to robotics offers a novel design methodology that eliminates the need of wiring between joints. However, like any evolving technology, QWiC is not without it challenges.

QWiC shares common problems with other WPT methods such as rectifier efficiency and receiver-side voltage regulation [4]. In addition, connecting a reactive load to the Quarter-Wave Resonator (QWR) that is inherent to QWiC alters the fundamental characteristics of the QWR, resulting in shifts in frequency, phase, and power traits within the system. These active loads diminish the quality factor (Q), particularly when connected in series, thereby reducing efficiency. This effect is amplified when directly connected in parallel [5]. Therefore any parameter changes that effect the electrical length of the QWR must be avoided while simultaneously not allowing power reflections at the load's input, a common issue in WPT systems [6]. Such issues make load regulation very difficult to achieve in applications where load variation is high, drive currents are large (such as a motor), and onboard energy storage is required. A balance must be made between charging rate and energy storage.

To address these challenges with QWiC systems, a high capacity power converter circuit is presented that enables the isolation of the converter from the QWR, while offering higher instantaneous drive currents in tandem with onboard energy storage. A control scheme is developed that implements secondary side sensing and regulation that is specifically designed for use in QWiC systems. The work here focuses on the trade-offs between energy storage and charging/discharging rates to enable high torque motor drive for a novel QWiC robotic prototype.

II. Capacitance

The proposed circuit topology for this work is shown in Fig. 1. The control signal (CTRL) is supplied from a microcontroller that measures the state of charge of C_1 and then controls the switching states utilizing a galium nitride transistor (GAN2). GAN1 forms a linear regulator which sets the maximum voltage that storage capacitance (C_1) can obtain. Fig. 1b is an equivalent model for State 1 when charging, while Fig. 1c is the discharging State 2. During State 1, C_1 and load resistance (R_L) are placed in parallel, with the source modeled as an ideal current source. Using the total current, $I(t)$, leaving

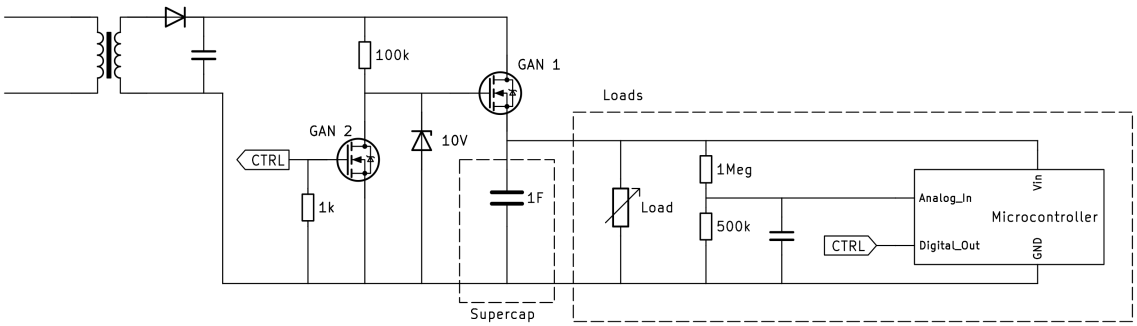

(a) Full Schematic

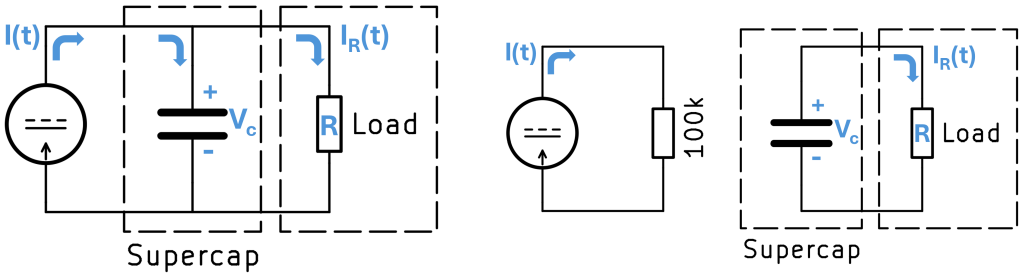

(b) State 1 **(c)** State 2

Figure 1: Schematic and Simplified States

the source and the current entering the load, $I_R(t)$, the voltage across the parallel node, V_C is found by,

$$V_c = \frac{1}{C_1}\int_0^T I(t) - I_R(t)\,dt \tag{1}$$

By rearranging and performing differentiation, we can represent the current function $I(t)$ in terms of the superposition of currents flowing through the load and capacitor (2).

$$I(t) = \frac{V_c}{R_1} + C_1\frac{dV_c}{dt} \Rightarrow V_c = R_1[I(t) - C_1\frac{dV_c}{dt}] \tag{2}$$

Therefore, the voltage across the capacitor depends on the input current's magnitude, the voltage's rate of change determined by capacitance (C_1), and is proportional to resistance (R_1). Higher voltage levels are attained by increasing the input current and load resistance or reducing the smoothing capacitance. One method to increase the input current on the secondary side involves amplifying the current on the primary side. In the case of a Quarter-Wave Resonator (QWR), the maximum current is concentrated at the coil's base [7]. Consequently, the transformer is positioned at the coil's base to optimize performance such as in Fig. 2.

When in the context of a QWiC system, this parallel load has higher voltages with high loads and lower voltages with low loads since the current is constant despite load. Experimentally this is shown in Fig. 3 on a 4.05 MHz coil. Notably, a higher load resistance increases Q, and a lower load resistance decreases Q.

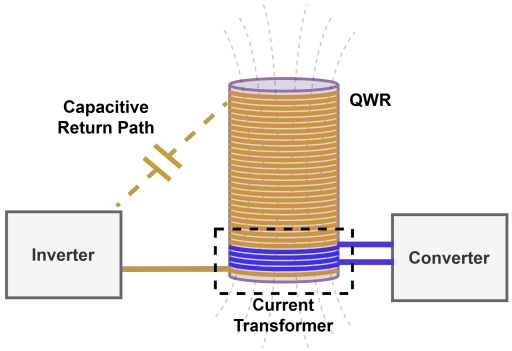

Figure 2: Converter Connection To QWiC System

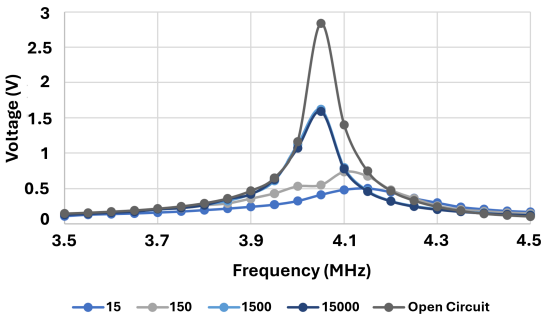

Figure 3: Frequency response under different loads in Ohms

Some loads can quickly change resistance, such as a motor that is intermittently operated. When the motor is activated,

the equivalent R_L will greatly reduce, forcing the storage capacitance C_1 to source the power to the motor, subsequently reducing V_c. Eventually V_c will reduce below the operating voltage of the various components that are fed by V_c, such as the motor, microcontroller, GANFets, etc. A limit can be set on by the microcontroller to limit the drop on V_c. Additionally, this discharge should not happen too quickly, otherwise the motor will not turn. Increasing capacitance however, can improve the discharge rate by increasing the time of discharge. By sufficiently boosting capacitance, the voltage will charge and discharge more gradually, effectively resembling a "rechargeable battery." This characteristic is beneficial during periods when the QWR might detune due to external stimuli, causing power loss [8]. The control of the discharge rate via switching between State 1 and State 2 offers a unique way of maintaining higher torques on motors when the amount of input current from the WPT transfer is not large enough to operate the motor continuously. In such situations, the proposed circuit implementation allows pulsing of the motor such that the perceived R_L of the motor is higher, improving the power delivery to the motor by better matching the load impedance with the QWR's higher impedance output. By manipulating (2), the amount of charge, Q, stored in the C_1 capacitor can be shown (3).

$$Q = \tau[I(t) - \frac{dQ}{dt}] \tag{3}$$

By increasing τ, more energy can be stored in the capacitor, but with a trade-off of slower charging rates.

Due to this trade-off, there are two optimization strategies that can be presented. One is increasing the load resistance while charging, which is done by pulsing the load. The other is finding the optimum capacitance for both charging and discharging. When driving a motor and the associated electronics in this system, the best capacitance was found to be between 0.3F to 1F.

III. Switching Circuitry

As stated previously, Fig. 1a utilizes the on/off cycles of GAN2 to control V_C, while GAN1 allows the C_1 to initially charge (if at zero) but then sets a max voltage limit so as not to damage the capacitor and subsequent circuitry. Effectively, the circuit connects the capacitor to the input when charging, and disconnects it from the input when discharging. When the micro-controller's CTRL pin is low (or even unpowered), the left transistor (GAN 2) assumes a state of high impedance. Consequently, this sets the gate-source (GS) voltage of GAN1 to $V_D - V_C$, where V_D is the voltage drop across the zener diode (D_Z). This maintains GAN1 in an "ON" state unless GAN2 is turned on or until V_C reaches a voltage that is less than the V_{GS} of GAN1, forming a linear regulation if GAN2 is left in an OFF state.

Conversely, when the micro-controller's control pin outputs a high signal, GAN2 turns on, causing the gate of GAN1 to connect to ground, rendering the V_{GS} of GAN1 equal to $-V_C$, turning GAN1 off. Caution is to be taken to prevent this voltage from surpassing the maximum gate voltage of the transistors. C_1 is then disconnected from the input rectifier, allowing it to discharge into the load fully as in Fig. 1c.

This setup simplifies the implementation of micro-controller code, as illustrated in Fig. 4. In the diagram, the two states are toggled based on whether the measured capacitor voltage (Vin) is greater than or lower than the allowable error bounds (Max Voltage and Min Voltage). For enabling the micro-controller to read the C_1 state of charge, a high impedance voltage divider is applied to C_1 and the output of the voltage divider is connected to a Analog-to-Digital Converter (ADC) pin on the micro-controller. A code-based voltage limit is then set that is below the maximum limit maintained by the linear regulator. In this work, the linear-regulator had a max voltage limit of near 10V, while the code-limit was set to a voltage of 6 V to 8 V during the testing.

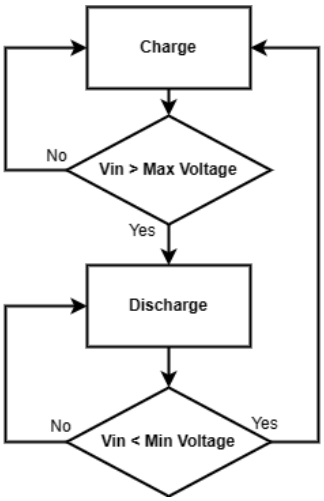

Figure 4: Micro-controller Flowchart

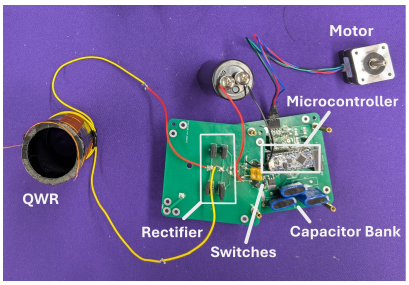

(a) Circuit Deconstructed and Annotated

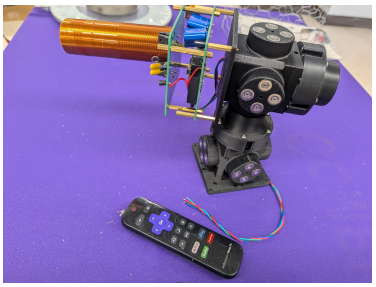

(b) Circuit Mounted to Modular Robot

Figure 5: Prototype

IV. Experimental Setup and Results

The experimental setup is photographed and annotated in Fig. 5a. The entire system when mounted is shown in Fig. 5b. PCBs were designed/fabricated with surface-mount components. The PCBs were stacked on top of each other and connected via metal standoffs. By connecting the ground planes with the standoffs, a Faraday cage is created isolating the DC components from the RF input to the rectifier.

An oscilloscope (Tektronix THS3014) was connected across the capacitor bank and the voltage was measured to show the State 1 charging of the circuit. The data is shown in Fig. 6. When a smaller capacitance was used, the charging rate was higher, with the circuitry beginning their regulation in a faster time-frame.

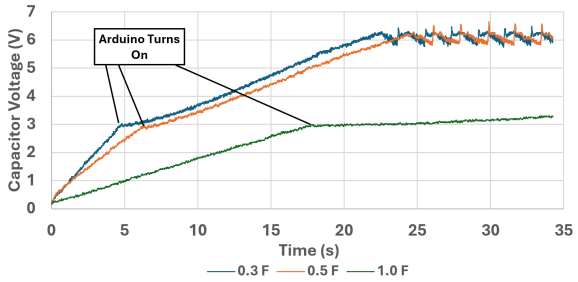

Figure 6: Voltage While Charging

Next, the capacitor voltage was measured as the motor was toggled. This showed an initial quick discharge before settling on around 4V. This is seen in Fig. 7. The motor functioned with a high torque output for approximately 1 second before it would lose torque. After this 1 second interval, V_C would be maintained at an equilibrium voltage that allowed the microcontroller to function, but the motor's torque was greatly reduced.

It can be seen in Fig. 7 that if the on duration of the motor was maintained below 1 second, it would be possible to pulse the motor on and off, allowing for the torque to be maintained without loss. Fig. 8 shows a modification to the code-based voltage limits that operate the motor for less than 1 second. The duty cycle is determined by the charge rate due to the RC time constant and discharge rate due to the motor.

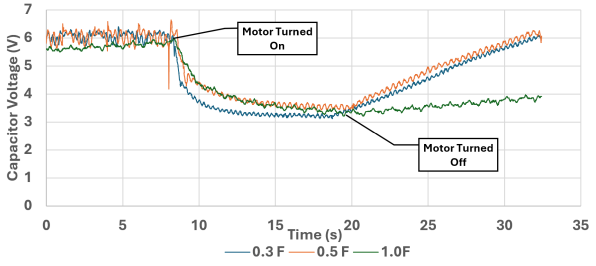

Figure 7: Voltage Response with a Continuously Applied Load Motor.

Both the capacitor voltage and the control signal from the micro-controller were recorded. This was able to show that the circuit did regulate based on the micro-controller output. As seen in Fig. 9, which uses 1F of capacitance, the circuit's voltage remained stable even with a switching frequency of roughly 0.125 Hz. By decreasing the allowable error, thus increasing the switching rate, more energy could theoretically be supplied as the recharge rate is faster than the discharge rate. However, the cost of the increased capacitance is the nearly minute-long charge time.

The voltage and current was measured at the input to determine operating power. An average of 6.9W was supplied during state 1. During state 2, the power is mostly reactive as the QWR is the only load, and only an average of 0.1W was supplied in active power.

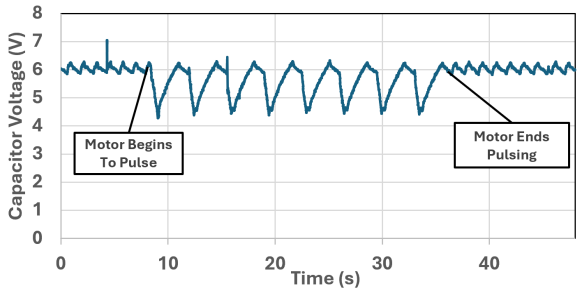

Figure 8: Voltage Response When Motor Is Pulse to Produce More Even Torque

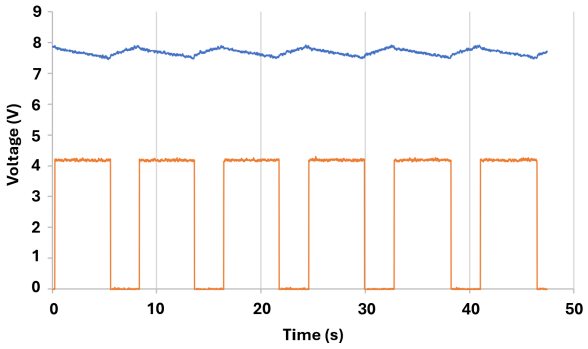

Figure 9: Regulated Voltage (Blue) and Micro-Controller Signal (Orange)

V. Conclusions and Future Work

A successful prototype of the proposed circuit was built and tested. The circuit successfully charged and regulated a digitally controlled reference voltage that was able to power a motor using QWiC power transfer, and a potential way to increase efficiency by pulsing the motor was quickly explored and showed promise.

References

[1] M. Z. Erel, K. C. Bayindir, M. T. Aydemir, S. K. Chaudhary, and J. M. Guerrero, "A comprehensive review on wireless capacitive power transfer technology: Fundamentals and applications," *IEEE Access*, vol. 10, pp. 3116–3143, 2022.

[2] L. Yang, Y. Zhang, X. Li, B. Feng, X. Chen, J. Huang, T. Yang, D. Zhu, A. Zhang, and X. Tong, "Comparison survey of effects of hull on AUVs for underwater capacitive wireless power transfer system and underwater inductive wireless power transfer system," *IEEE Access*, vol. 10, pp. 125 401–125 410, 2022.

[3] J. Dean, M. Coultis, and C. Van Neste, "Wireless sensor node powered by unipolar resonant capacitive power transfer," in *2021 IEEE PELS Workshop on Emerging Technologies: Wireless Power Transfer (WoW)*, 2021, pp. 1–5.

[4] E. Moisello, A. Liotta, P. Malcovati, and E. Bonizzoni, "Recent trends and challenges in near-field wireless power transfer systems," *IEEE Open Journal of the Solid-State Circuits Society*, vol. 3, pp. 197–213, 2023.

[5] C. W. Van Neste, A. Phani, A. Larocque, J. E. Hawk, R. Kalra, M. J. Banaag, M. Wu, and T. Thundat, "Quarter wavelength resonators for use in wireless capacitive power transfer," in *2017 IEEE PELS Workshop on Emerging Technologies: Wireless Power Transfer (WoW)*, 2017, pp. 229–234.

[6] K. Kusaka and J.-i. Itoh, "Input impedance matched AC-DC converter in wireless power transfer for EV charger," in *2012 15th International Conference on Electrical Machines and Systems (ICEMS)*, 2012, pp. 1–6.

[7] T. Marcrum, J.-C. Williams, C. S. Johnson, M. Pearce, C. Pope, C. W. Van Neste, C. Vaughan, and D. Boyd, "Quasi-wireless capacitive power transfer for wire-free robotic joints," *Energies*, vol. 17, no. 12, 2024. [Online]. Available: https://www.mdpi.com/1996-1073/17/12/2858

[8] C. A. Robinson, M. G. S. Pearce, H. Lu, and C. W. Van Neste, "Capacitive omnidirectional position sensor using a quarter wave resonator," *IEEE Sensors Journal*, vol. 22, no. 16, pp. 15 817–15 824, 2022.